DOI: 10.1002/anie.201206410

Proton-Conducting Materials

Proton Conduction in Metal–Organic Frameworks and Related Modularly Built Porous Solids

Minyoung Yoon, Kyungwon Suh, Srinivasan Natarajan, and Kimoon Kim**

coordination polymers · fuel cells · metal–organic frameworks · porous materials · proton conduction

Proton-conducting materials are an important component of fuel cells. Development of new types of proton-conducting materials is one of the most important issues in fuel-cell technology. Herein, we present newly developed proton-conducting materials, modularly built porous solids, including coordination polymers (CPs) or metal–organic frameworks (MOFs). The designable and tunable nature of the porous materials allows for fast development in this research field. Design and synthesis of the new types of proton-conducting materials and their unique proton-conduction properties are discussed.

1. Introduction

The increasing energy demands of the world impart serious constraints on the available natural resources such as oil and gas. There have been considerable efforts in identifying alternate energy sources, of which solar energy figures prominently. In the heart of the search for other useful sources of energy, chemistry could play an important role. Conversion of chemical energy into other useable forms has been known since the time of Volta.[1] Harvesting solar energy using chemical antennas has been in vogue in recent years.[2] In addition to these, the usefulness of fuel cells appears to be an attractive option as an alternative energy converting system for utilization of alternative energy sources, such as hydrogen and methanol. The considerable effort devoted to developing this approach has resulted in many types of fuel cell technologies.[3] Of these, the hydrogen fuel cell is important. In the anode of hydrogen fuel cells, electrons are drawn from hydrogen to produce protons. The electrons, then, are transferred to a cathode of the fuel cell through an external circuit producing direct current. The protons are transported across a permeable membrane to the cathode converting the chemical energy into electrical energy. The product of the chemical reaction is water and heat, thus making this technology clean with regard to the environmental issues. The beneficial aspects of the fuel cell have prompted many researches to look for materials that can transport protons efficiently, as the facile proton conduction appears to be at the heart of the fuel-cell technology. The proton transfer processes, including those in plants for photosynthesis, have been studied with great interest for diverse applications by chemists, physicists, and biologists. The most studied and explored proton-conducting materials are based on polymers, such as Nafion, which works efficiently in the presence of water and at temperatures lower than 80 °C.[4] Though the use of Nafion or Nafion-like polymer membranes are attractive, the high cost of the membranes still prevent a large-scale use in many technologies. Development of cheaper and yet better-performing polymeric materials has been thus a subject of intense research.[4b]

Over the years, researchers have explored many other materials, in addition to the polymeric ones, such as sulfonated polyether ketone, oxo acids, oxides, hydroxides, apatites, and inorganic–organic hybrids as possible candidates for proton conductivity.[5] Proton-conductivity studies were recently extended to porous solids, such as mesoporous silica, coordination polymers (CPs) or metal–organic frameworks (MOFs),[6,7] and organic porous solids[8] with reasonable results.

Recently, portable fuel cells, miniature fuel cells that are transportable, have been used to power many everyday electronic devices, such as laptop computers and cellular phones, which operate at low temperature. Although Nafion and polymeric materials have been widely used in fuel cells operating at low temperature, development of new conduct-

[*] Dr. M. Yoon, K. Suh, Prof. Dr. S. Natarajan, Prof. Dr. K. Kim
Division of Advanced Materials Science, Center for Smart Supramolecules, and Department of Chemistry
Pohang University of Science and Technology (Republic of Korea)
E-mail: kkim@postech.ac.kr
Homepage: http://css.postech.ac.kr
Prof. Dr. S. Natarajan
Permanent address: Framework Solids laboratory, Solid State and Structural Chemistry Unit, Indian Institute of Science
Bangalore-560012 (India)
E-mail: snatarajan@sscu.iisc.ernet.in
Homepage: http://sscu.iisc.ernet.in/frameworkslab/

ing materials having higher proton conductivity (over 0.1 $S\,cm^{-1}$) and operating in a wider temperature range (25–300 °C) is required to increase the efficiency of fuel cells. Modular porous materials, such as MOFs and organic porous materials, attract much attention as they may meet these requirements. Herein, we will briefly touch on the history of proton-conducting solids and focus on the development of proton-conducting modular porous solids, especially MOFs and organic molecular porous solids.

2. Brief History of Proton Conduction in Solids

Proton conductivity can be considered to be a special case of ionic transport, in that the transporting ion is small not even possessing an electronic shell. The existence of protonic species in aqueous solution was shown through the pioneering work of Grotthuss.[9] The earliest documented study of proton transport could be traced to the investigation of electrical transport in ice.[10] After the initial study, Bjerrum,[11] Eigen and co-workers[12] expanded the scope of proton conduction in ice, which can be considered as the first systematic study of proton conduction in solids.[13] Since then, water-mediated proton conductivity has been widely studied.[14]

The first proton-conducting material exploited for applications was the perfluorinated sulfonated polymer, commercially known as Nafion, discovered at DuPont in the 1960s.[15] Proton-conducting membranes based on Nafion were used in the early space programs, such as the Gemini and Apollo programs. Following Nafion, a number of similar polymers have been developed,[16] which operate in a temperature range of 20–80 °C with a high conductivity (ca. 10^{-2} $S\,cm^{-1}$),[17] but quickly lose proton conductivity above 80 °C upon loss of water molecules.

Persistent research during the 1970s and 1980s led to the discovery of a number of proton-conducting materials including salts without acid protons, acid salts, organic acids, hydrates, hydrogen-bonded molecular compounds, and organic polymers.[5a,18] Of these, the ceramic oxides are important.[19] Extensive work by Takahashi and Iwahara,[20a] Kreuer[20b] led to the discovery of proton-conducting oxides, based on the perovskite structure, as well as elucidation of the proton-conduction mechanism in them. The defect chemistry of the rare-earth oxides were exploited for the study of proton conduction in the early 1990s.[21] Generally, ceramic oxides operate at a very high temperature (600–1000 °C) and show a conductivity range of 10^{-2}–10^{-6} $S\,cm^{-1}$.

High proton conductivity has also been observed in many oxo acids and their salts, such as phosphoric acid and $CsHSO_4$.[5b] Oxo acids dissociate in aqueous solution, generating hydrated protons for proton conduction. Such acids may show appreciable proton conductivity (e.g., H_3PO_4,[22] H_3OClO_4)[23] even in the absence of water as a result of their self-dissociation.[24] Solid oxo acid salts, such as $MHXO_4$ (M = Rb, Cs) have chemical properties between those of an acid and a salt, making them potential candidates as proton-conducting materials.[25] Solid acids undergo a structural change at temperatures above 120 °C leading to a highly conducting phase. Solid acids generally work at an intermediate temperature (120–300 °C) with high proton conductivity (10^{-2}–10^{-5} $S\,cm^{-1}$).

The earliest study of proton conductivity in hydrogen-bonded (H-bonded) systems was on the acid–base salts of mineral acids and organic bases. The salts of sulfuric acid and triethylenediamine and hexamethylenetetramine have been

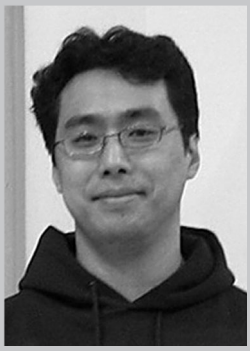

Minyoung Yoon received a B.S. degree and Ph.D. degrees in chemistry under the supervision of Professor Kimoon Kim from POSTECH in 2005 and 2011, respectively. He is currently a postdoctoral research fellow at POSTECH. His current research focuses on applications of novel porous materials for catalysis, gas separation, and ion conduction.

Kyungwon Suh recieved a B.S. degree in Chemistry from Kyungbook National University in 2006. He is currently a Ph.D. student with Professor Kimoon Kim at POSTECH. His research focuses on energy conversion and storage using porous materials and carbonized porous materials.

Srinivasan Natarajan obtained his Ph.D degree from the Indian Institute of Technology, Madras (1990). After postdoctoral work at the Royal Institution of Great Britain, UK and University of California, Santa Barbara, he joined the Jawaharlal Nehru Center for Advanced Scientific Research in 1997. He moved to the Indian Institute of Science, Bangalore in 2004, where he is a Professor. His research interests are in solid state and materials chemistry, especially in functional inorganic solids with open structures. This Minireview was written on his sabbatical at POSTECH.

Kimoon Kim studied chemistry at Seoul National University (B.S., 1976), KAIST (M.S., 1978), and Stanford University (Ph.D., 1986). After postdoctoral work at Northwestern University, he joined Pohang University of Science and Technology where he is now Distinguished University Professor. Recently, he has been appointed as director of the Center for Self-assembly and Complexity (CSC), Institute for Basic Science (IBS). His current research focuses on developing novel functional materials and systems based on supramolecular chemistry.

investigated for proton-conducting behavior.[26] The blends of oxo acids and a variety of polymers were also studied for proton conductivity during the early 1990s.[27] Most of the hydrogen-bonded acid–base systems work below 80 °C with moderate proton conductivity (10^{-4}–10^{-6} S cm^{-1}).

Polybenzimidazole membranes impregnated with phosphoric acid (PBI) drew much attention because of their intermediate operation temperature (80–200 °C) as well as proton conductivity values comparable to Nafion (ca. 10^{-2} S cm^{-1}). Recently, several derivatives of the PBI copolymers along with other strong acid additives, such as organic sulfonates, have been investigated for proton conductivity.[28] In the search for materials that can exhibit high proton conductivity, heterocyclic organic molecules, such as imidazole and pyrazole, were employed as an additive in polymers. Intercalation or polymerization of such organics within the lamellar structures provided new materials with interesting proton conducting behavior.[29] In addition, heteropolyacids (HPA) with Keggin anion structures as composite membranes on silica supports[30] and PBI supports[31] have been studied. Such composite solids show proton conductivity values (0.1 S cm^{-1}) comparable to that of Nafion. The proton conductivity, however, drops substantially at temperatures above 80 °C, similar to Nafion.

The rapid development of MOFs,[6] inorganic–organic hybrid materials with well-defined pores and channels, since late 1990s, opened up exciting new opportunities in proton-conducting materials. Two different types of proton-conducting MOFs have been studied, water-mediated proton-conducting MOFs and anhydrous proton-conducting MOFs. The water-mediated form operate at a low temperature (20–80 °C) with proton conductivity ranging between 10^{-2} and 10^{-8} S cm^{-1}, whereas the anhydrous form works at an intermediate temperature (100–250 °C) with proton conductivity ranging between 10^{-2}–10^{-6} S cm^{-1}. Figure 1 summarizes the proton conductivity of various proton-conducting materials including MOFs and their operating temperatures.[32]

The crystalline nature of MOFs allows precise determination of their structures at the atomic level. The structural information of MOFs provides a useful insight into the proton-conduction pathway and mechanism, which may be useful in designing new proton-conducting materials. In addition, the tunability of MOF structures and properties provides an opportunity to control the proton-conduction properties, which may be useful in developing sensor and other devices. Herein, we highlight the developments in new MOF-based proton-conduction materials and related materials.

3. Measurements of Proton Conduction in MOFs

Until recently, most of proton conductivities of MOFs and related modular porous materials have been measured by the two-probe (quasi-four probe) or four-probe method of AC impedance spectroscopy[33] using compacted pellets of powdered samples. Although proton-conductivity measurements using pellets are useful to provide the macroscopic proton conductivity of a material, it often fails to reveal its intrinsic proton conductivity due in part to the presence of grain boundary. More serious limitation of the "pellet" measurements is that they do not provide information on the anisotropy in conductivity, although MOF-based proton conductors have often highly anisotropic structures. Very recently, therefore, people started to use single-crystal proton-conductivity measurements to study the intrinsic proton conductivity including directional or anisotropic proton conductivity. Typically, the proton conductivity ob-

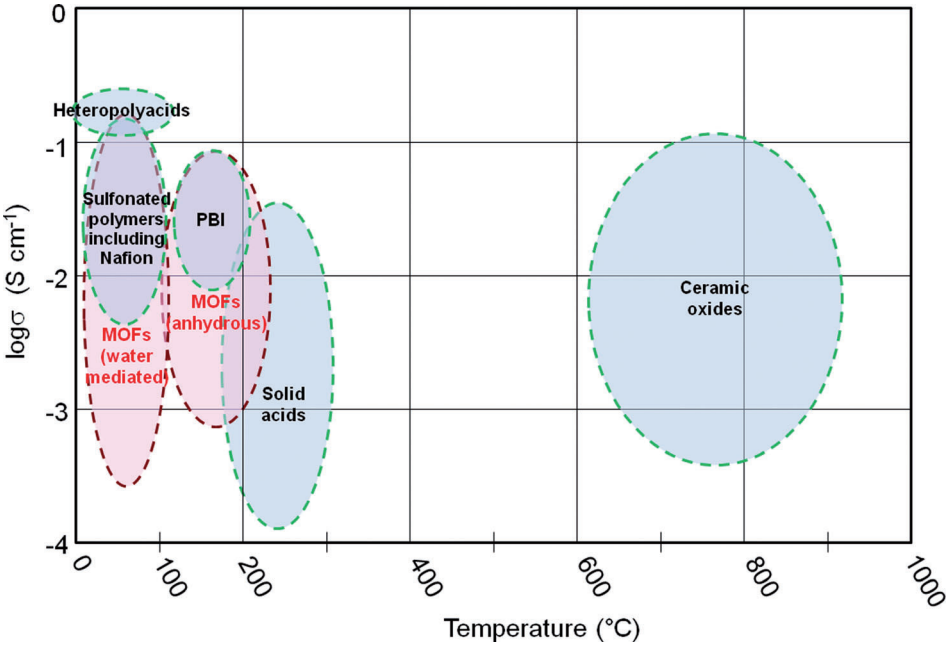

Figure 1. Conductivity of various proton-conducting solids and their operating temperatures.[32]

tained by single-crystal measurements is one or two orders of magnitude higher than that obtained by powder measurements. Furthermore, anisotropic proton conduction was observed in several single crystals with a conductivity ratio $\sigma_{\parallel}/\sigma_{\perp}$ as large as 10^4.[34] In combination with X-ray single-crystal structures, proton-conductivity measurements using single-crystals provide important clues towards understanding the possible mechanism as well as proton-conduction pathways in MOF-based proton conductors.

4. Proton Conduction in MOFs

Proton-conducting properties of coordination polymers (CPs) were first demonstrated by Kanda and co-workers in late 1970s with a two-dimensional (2D) MOF, [*N*,*N*′-bis(2-hydroxyethyl)dithiooxamido]copper(II), $[(HOC_2H_4)_2$-(dtoa)Cu].[35] However, they received little attention until recently. With the rapid developments in MOF research since the 1990s, their applications in gas storage,[36] separation,[37] catalysis,[38] and magnetism,[39] have been extensively explored. In addition, with the renewed interests in fuel cells and related applications in recent years, the potential of MOFs as proton-conducting materials became evident (see Table 1), as MOFs can provide precisely designed frameworks with pores and channels, in which various conducting media, such as water molecules, are included to serve as proton-conduction pathways.

Proton conducting MOFs can be divided into two categories, water-mediated proton-conducting MOFs (containing water-mediated hydrogen bonding networks serving as a proton conduction pathway) and anhydrous (or non-

Table 1: Proton-conducting MOFs and related modularly constructed porous solids.

Compound	Conductivity [S cm^{-1}]	Activation energy [eV]	Measurement condition	Reference
Water-mediated proton-conducting MOFs				
Fe(ox)·2 H_2O (**1**)[a]	1.3×10^{-3}	0.37	25 °C, 100% RH	[40]
[Mn(dhbq)·H_2O] (**2**)[b]	4×10^{-5}	0.26	RT, 98% RH	[41]
$[Mo_5P_2O_{23}][Cu(phen)(H_2O)]_3$·5 H_2O (**3**)[c]	2.2×10^{-5}	0.23	28 °C, 98% RH	[42]
In-5TIA (**4**-In)	5.35×10^{-5}	0.14	28 °C, 98% RH	[43]
Cd-5TIA (**4**-Cd)[d]	3.61×10^{-3}	0.16	28 °C, 98% RH	[43]
$[(HOC_2H_4)_2(dtoa)Cu]$ (**5**)[e]	5×10^{-6}	0.16	25 °C,100% RH	[45]
$(NH_4)_2(adp)[Zn_2(ox)_3]$·3 H_2O (**6**)[f]	8×10^{-3}	0.63	25 °C, 98% RH	[48]
{NH(prol)$_3$}[MCr(ox)$_3$] (**7**)[g]	$\approx1\times10^{-4}$	n/a	25 °C, 75% RH	[49]
$[NMe_3(CH_2CO_2H)][FeCr(ox)_3]$ (**8**)	0.8×10^{-4}	n/a	RT, 65% RH	[50]
$(NH_4)_4[MnCr_2(ox)_6]$·4 H_2O	1.1×10^{-3}	0.23	RT, 96% RH	[51]
PCMOF-3 (**9**)[h]	3.5×10^{-5}	0.17	RT, 98% RH	[53]
Fe(OH)(bdc-COOH) (**10**-COOH)	2.0×10^{-5}	0.21	25 °C, 95% RH	[55]
HKUST-1-H_2O (**11**-H_2O)[i]	1.5×10^{-5}	n/a	RT, methanol vapor	[58]
$Co[Cr(CN)_6]_{2/3}$·4.8 H_2O (**12**-Co)	1.2×10^{-3}	0.22	20 °C, 100% RH	[59]
$[Zn(l\text{-}L_{Cl})(Cl)]$·$H_2O$ (*l*-**13**)[j]	4.45×10^{-5}	0.35	30 °C, 98% RH	[60]
Anhydrous proton-conducting MOFs				
Im@Al(μ_2-OH)(1,4-ndc) (im@**14**)[k]	2.2×10^{-5}	0.6	120 °C, anhydrous	[61]
Im@Al(μ_2-OH)(1,4-bdc) (im@**15**)[k]	1.0×10^{-7}	0.9	120 °C, anhydrous	
His@Al(μ_2-OH)(1,4-bdc) (his@**15**)[m]	1.7×10^{-3}	0.25	150 °C, anhydrous	[63]
Tz@β-PCMOF-2 (Tz@**16**)[l]	$2\text{-}5\times10^{-4}$	0.34–0.60	150 °C, anhydrous (H_2)	[64]
$[Co_2Na(bptc)_2][Emim]_3$ (**17**)[n]	6.6×10^{-7}[o] $\sigma_{[100]}=2.6\times10^{-5}$, $\sigma_{c\text{-axis}}=4.8\times10^{-7}$	n/a	170 °C RT (single crystal)	[67]
$[Zn(H_2PO_4)_2(TzH)_2]$ (**18**)	1.2×10^{-4} $\sigma_{\parallel}=1.4\times10^{-4}$, $\sigma_{\perp}=2.9\times10^{-6}$	0.6	150 °C, anhydrous 130 °C (single crystal)	[68]
Proton-conducting organic molecular porous solids				
Quinuclidine–thiourea (**19**)	10^{-5} - 10^{-11} $\sigma_{\parallel}=2.2\times10^{-4}$, $\sigma_{\perp}=2.4\times10^{-6}$	n/a	atmospheric condition RT (single crystal)	[69]
CB[6]·H_2SO_4 (**20**)[p]	1.3×10^{-3} $\sigma_{\parallel}=4.3\times10^{-2}$, $\sigma_{\perp}=5.0\times10^{-6}$	0.31	25 °C, 98% RH RT (single crystal)	[34]
CB[6]·HCl (**21**)[p]	1.1×10^{-3} $\sigma_{\parallel}=2.4\times10^{-2}$, $\sigma_{\perp}=7.1\times10^{-5}$	0.39	25 °C, 98% RH RT (single crystal)	[34]

[a] ox = oxalate. [b] dhbq = 2,5-dihydroxy-1,4-benzoquinone. [c] phen = phenanthroline. [d] TIA = 5-triazole isophthalic acid. [e] dtoa = dithiooxamido. [f] adp = adipate. [g] prol = 3-hydroxypropyl. [h] PCMOF-3 = $Zn_3(L)H_2O$·2 H_2O, L = 1,3,5-tribenzenetriphosphonate. [i] HKUST-1 = $Cu_3(btc)_2$, btc = benzenetricarboxylate. [j] *l*-L_{Cl} = 3-methyl-2-(pyridin-4-ylmethylamino)-butanoic acid. [k] Im = imidazole; 1,4-ndc = 1,4-naphthalenedicarboxylate; 1,4-bdc = 1,4-benzenedicarboxylate. [l] Tz = triazole. [m] His = histamine. [n] bptc = 2,2′,4,4′-biphenyl tetracarboxylate; Emim = 1-ethyl-3-methylimidazolium. [o] σ along the *c*-axis of single crystal. [p] CB[6] = cucurbit[6]uril.

water-mediated) proton-conducting materials which have water-free proton conduction pathways. In the following Sections, we describe the two different types of proton-conducting MOFs and their proton-conduction behavior.

4.1. Water-Mediated Proton Conducting MOFs

In general, low-temperature proton-conducting materials rely on the presence of water molecules and the hydrogen-bonding interactions of the water molecules playing an important role in the migration of protons. In water-mediated proton-conducting MOFs or CPs, the structure of the hydrogen-bonding networks, which serve as proton-conduction pathways, is usually dictated by the structure or dimensionality of the frameworks. In describing water-mediated proton-conducting MOFs, therefore, we categorized them into 1D CPs, 2D MOFs, and 3D MOFs depending on the framework structure.[7]

4.1.1. Proton-Conducting 1D Coordination Polymers

There are only a few examples of 1D CPs investigated for proton conduction.[40,41] Among them, ferrous oxalate (ox) dihydrate (Humboldtine), $Fe(ox)\cdot 2H_2O$ (**1**), is important.[40] Oxalate connects two Fe^{II} ions by coordination to the equatorial positions of Fe^{II} centers, resulting in the formation of 1D chains (Figure 2a).

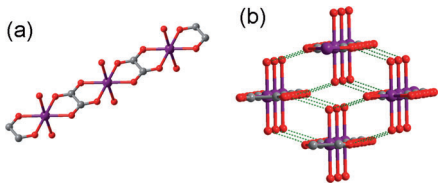

Figure 2. a) 1D chain structure of **1** and b) perspective view of **1**, hydrogen bonding is shown as green dashed lines. Fe purple, O red, C gray.

Two axial positions of the Fe^{II} center are coordinated by water molecules that are arranged in such a way to form strong hydrogen bonds with the framework oxalate oxygen atoms (O···O 2.71 Å), which would provide a pathway for proton conduction (Figure 2b). Proton conductivity was measured to be $1.3\times10^{-3}\,S\,cm^{-1}$ with an activation energy of 0.37 eV at room temperature (RT) and 98% relative humidity (RH).[40] Similar studies have also been carried out on other 1D CPs, such as $M(dhbq)\cdot 2H_2O$ (**2**), where M = Mg, Mn, Co, Ni and Zn; $H_2(dhbq)$ = 2,5-dihydroxy-1,4-benzoquinone.[41] However, their proton conductivity is considerably lower ($<4\times10^{-5}\,S\,cm^{-1}$) than that of **1**. The anhydrous form of **2** did not exhibit any proton conductivity, suggesting that the proton conduction occurs because of the presence of the coordinated water molecules.

A polyoxometalate (POM) based 1D CP, $[Mo_5P_2O_{23}][\{Cu(phen)(H_2O)\}_3]\cdot 5H_2O$ (**3**), was investigated for proton-conduction properties. In **3**, two $[Mo_5P_2O_{23}]^{6-}$ clusters are connected by a Cu(phen) unit to form a 1D chain along the crystallographic *a* axis.[42] The 1D chains are interdigitated by π–π stacking of the phenanthroline rings, which holds five non-coordinated water molecules forming a 1D hydrogen-bonded water chain between the stacked coordination polymer 1D chains. It exhibited proton conductivity of $2\times10^{-5}\,S\,cm^{-1}$ with an activation energy of 0.23 eV at 28 °C and 98% relative humidity. The proton conductivity showed a direct correlation with the relative humidity, decreasing with decreasing humidity. The proton conductivity was lost at 42 °C, presumably because of disorder in the arrangement of the water molecules.

Very recently, a new type of 1D proton-conducting material, single-walled, functionalized metal–organic nanotubes (MONTs), was reported. (Figure 3a).[43] The 1D MONTs, In-5TIA (**4**-In), and Cd-5TIA (**4**-Cd), containing triazole functionalized isophthalic acid (5TIA) have an isostructural tubular structure decorated by free triazole moieties on the outer surface of the tubes, which form a complex hydrogen bonding pattern with ammonium ions and water molecules. They showed proton conductivity of $5.35\times10^{-5}\,S\,cm^{-1}$ and $3.61\times10^{-3}\,S\,cm^{-1}$, respectively, at 28 °C and 98% relative humidity. The low activation energy (0.14 eV and 0.16 eV, respectively) of the proton conduction in **4**-In and **4**-Cd suggests that the proton probably hops along the hydrogen-bonding network in the nanotubes (Figure 3b).

4.1.2. Proton-Conducting 2D Metal–Organic Frameworks

As briefly described above, the first study of proton conduction in CPs or MOFs was reported by Kanda et al. using a series of copper dithiooxamides with a 2D network structure.[35,44] Of them, [*N*,*N*′-bis(2-hydroxyethyl)dithiooxamido] copper(II), $[(HOC_2H_4)_2(dtoa)Cu]$ (**5**), is a semiconductor and exhibits both electronic as well as the ionic conduction. Proton conductivity of $5\times10^{-6}\,S\,cm^{-1}$ at room temperature and 100% relative humidity, was observed. At this humidity level, **5** holds about 10 water molecules between the 2D sheets, similar to Nafion.[45] However, the proton conductivity drops approximately 3 orders of magnitude at 45% relative humidity.[46a] Many variations on the above compounds have been prepared, by substituting the hydroxy ethyl group, and investigated for proton conductivity.[46] Regardless of the substituting functional groups, the derivatives showed similar proton conductivity in the range 10^{-5}–$10^{-6}\,S\,cm^{-1}$. Although the proton conductivity of the 2D MOFs was low compared to other materials, such as Nafion, this was the first systematic study on proton conduction in MOFs or CPs.

Oxalate complexes of divalent 3d metal ions generally form 2D-layered structures and the inter-lamellar space can be easily manipulated to create interesting magnetic properties in the compounds.[47] Zinc oxalate containing both ammonium as well as adipic acid (adp), $(NH_4)_2(adp)$-$[Zn_2(ox)_3]\cdot 3H_2O$ (**6**), has a classical 2D honeycomb network formed by Zn^{2+} and oxalate units (Figure 4a).[48] The structure containing H_2O, NH_4^+, and adipic acid moieties within the interlayer spaces (Figure 4a,b) exhibits strong

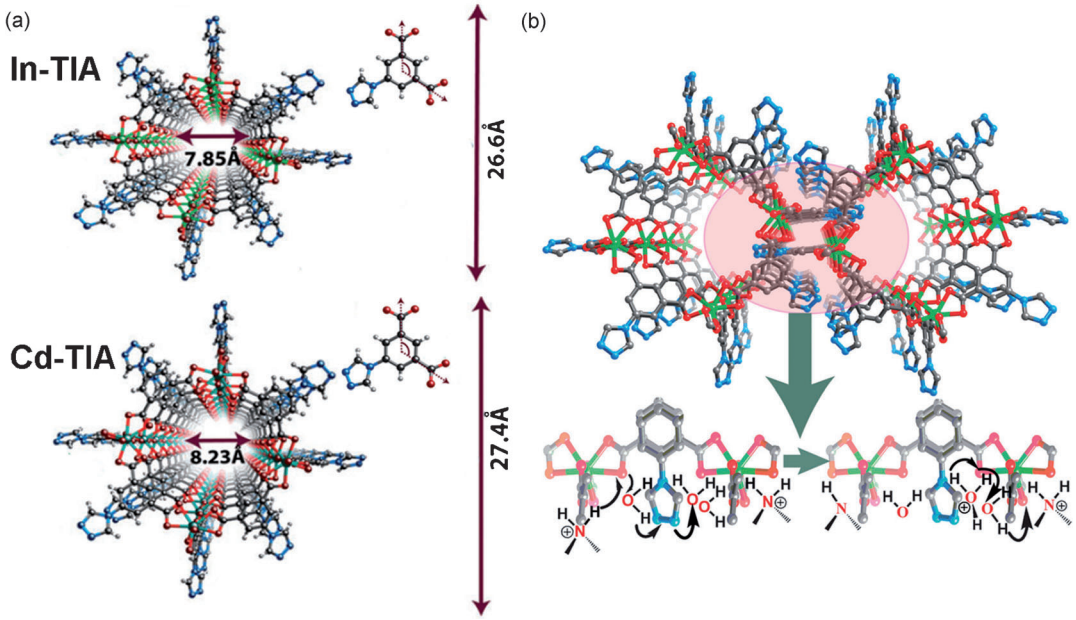

Figure 3. a) Structure of **4**-In (top) and **4**-Cd (bottom) MONTs (insets: 5-triazole isophthalic acid) and b) schematic representation of the proton-hopping mechanism along 1D nanochannels for **4**-In and **4**-Cd.[43] O red, N blue, metal green.

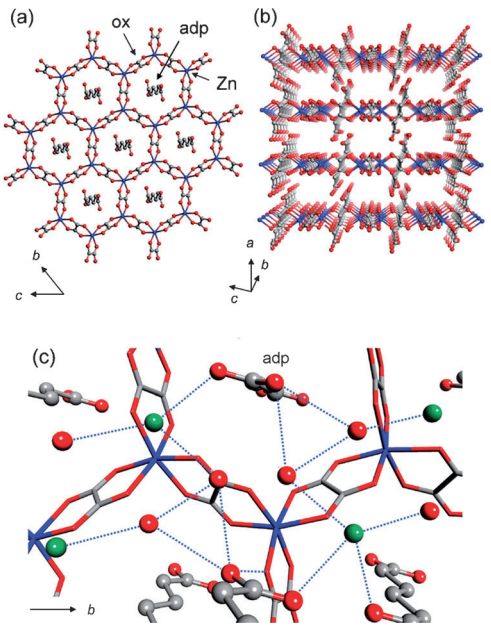

Figure 4. a) Honeycomb layer structure of **6**. b) Perspective view along the *b* axis. c) Hydrogen-bond arrangements (blue dotted lines) of -COOH, H_2O, and NH_4^+ in the interlayer spaces;[48] Zn blue, O red, C gray, N green.

hydrogen-bonding interactions involving all the guest molecules and the host oxalate units (Figure 4c). The proton conductivity of **6** was measured to be 8×10^{-3} S cm^{-1} at 25 °C and 98 % relative humidity and decreased to 6×10^{-6} S cm^{-1} at 70 % relative humidity. The strong humidity dependence of conductivity suggests that the water molecules present in the interlayer spaces are important for the proton conduction.

Related oxalate-based MOFs containing other guest molecules, such as tris(3-hydroxypropyl)ammonium, $[NH(prol)_3]^+$, $[NH(prol)_3][MCr(ox)_3]$ (**7**), M = Mn^{II}, Fe^{II}, Co^{II}, have been investigated for proton conduction.[49] They have lower proton conductivity (1×10^{-4} S cm^{-1}) and exhibit similar humidity dependency. Interestingly, all the bimetallic oxalate complexes also showed ferromagnetism at low temperature (T_C = 5–10 K). Thus, these compounds represent the first examples of the coexistence of magnetism and protonic conduction in solids. In addition, exchange of the guest ammonium ions in **7**, with $\{NR_3(CH_2COOH)\}^+$, where R = Me (methyl), Et (ethyl), or Bu (*n*-butyl), allowed control of the hydrophilicity of the lining of the pores, resulting in the control of the proton conductivity of the materials.[50] The proton conductivity of the MOFs increased with increasing hydrophilicity of the cations. The framework containing the most hydrophilic cation, $[N(CH_3)_3(CH_2COOH)][FeCr(ox)_3]$ (**8**), adsorbed the largest number of water molecules showing the highest proton conductivity of 0.8×10^{-4} S cm^{-1}, even at a low humidity (65 % relative humidity) and ambient temperature. This is the highest conductivity among proton-conducting MOFs operating under low humidity (below 70 % relative humidity) and the first example of water uptake control by modifying hydrophilicity of guest molecules, resulting in the control of proton conductivity. Related to these studies, a new bimetallic oxalate MOF, $(NH_4)_4[MnCr_2(ox)_6]\cdot4H_2O$, having a 3D chiral quartz-like structure was recently reported to show high proton conductivity (1.1×10^{-3} S cm^{-1}).[51]

Two-dimensional MOFs composed of phosphonate-containing ligands can offer a unique opportunity because phosphonates contain three oxygen atoms that can act as proton accepters.[52] The 2D-layered compound, $Zn_3(L)H_2O\cdot2H_2O$ (**9**) [L = (1,3,5-benzenetriphosphonate)$^{6-}$],

(PCMOF-3) was examined for possible proton conduction.[53] The coordinated water molecules on the Zn center point towards the interlayer space, which, along with the free lattice water molecules make the interlayer space highly hydrophilic. The extensive hydrogen bonding between the water molecules (free as well as coordinated) and the phosphonate oxygen atoms provides a conduit for proton conduction. The studies revealed a proton conductivity of 3.5×10^{-5} S cm^{-1} and an activation energy of 0.17 eV at room temperature and 98% relative humidity. As expected, **9** exhibited humidity-dependent proton conductivity, 4×10^{-8} S cm^{-1} at 44% relative humidity.

4.1.3. Proton-Conducting 3D Metal–Organic Frameworks

MOFs having three-dimensionally extended structures have also been investigated for proton conductivity. H. Kitagawa and co-workers reported the control of proton conductivity by incorporation of different functional groups at the ligands forming the MOFs. A significant variation in the proton conducting properties (Table 2) was observed in a family of isostructural 3D MOFs, M(OH)(bdc-R) (MIL-53),[54] [bdc = 1,4-benzenedicarboxylate; M = Al for R = H (**10**), NH_2 (**10**-NH_2), OH (**10**-OH) and M = Fe for R = $(COOH)_2$ (**10**-COOH).[55] A major factor to control the proton conductivity in this system is the acidity of the functional groups. The pK_a values of *meta*-substituted benzoic acids (R = NH_2, H, OH, and COOH) are 4.74, 4.19, 4.08, and 3.62, respectively,[56] which directly correlate with the order of the measured proton conductivity and activation energy of the materials (Table 2). This is the first example demonstrating that proton conductivity can be readily controlled by introducing different functional groups inside the pores of MOFs.

Table 2: Proton conductivities at 298 and 353 K under 95% relative humidity and activation energies for **10** and its derivatives.

Compound	σ [S cm^{-1}]		E_a [eV]	pK_a
	298 K	353 K		
10	2.3×10^{-8}	3.6×10^{-7}	0.47	4.19
10-NH_2	2.3×10^{-9}	4.1×10^{-8}	0.45	4.74
10-OH	4.2×10^{-7}	1.9×10^{-6}	0.27	4.08
10-COOH	2.0×10^{-6}	0.7×10^{-5}	0.21	3.62

Very recently, Hupp and co-workers investigated the proton conductivity of HKUST-1 (**11**),[57] a 3D MOF built on Cu paddle wheels at the nodes and 1,3,5-benzenetricarboxylate linkers.[58] Each Cu ion at the nodes has an open coordination site initially occupied by solvent molecules (both H_2O and ethanol), which can be exchanged with a variety of other solvent molecules including methanol, ethanol, CH_3CN, and H_2O by post-synthetic modification. Incorporation of water molecules on the open coordination site of **11** (**11**-H_2O) led to a large (ca. 75-fold) enhancement in proton conductivity (1.5×10^{-5} S cm^{-1}) under methanol vapor which fills the pores, relative to **11**-CH_3CN containing acetonitrile molecules coordinated to the Cu at the nodes. The enhanced conductivity was ascribed to the enhanced proton donation to methanol by coordinated water, as the pK_a value of water molecules decreased by coordination to the metal center. In contrast, when **11**-H_2O was exposed to *n*-hexane vapor, **11**-H_2O yielded a limiting conductivity more than five orders of magnitude lower than that of **11**-H_2O under methanol vapor. Although the study was limited to several variants of HKUST-1, this new approach provides important clues to tailoring the proton conductivity in porous solids.

Other important proton-conductivity studies have been carried out on Prussian blue analogues with a 3D framework structure (Figure 5a). Proton conductivity of two Prussian blue analogues, M[Cr(CN)$_6$]$_{2/3}$·*x*H_2O (M = Co and V and *x* = 4.8 for Co and 4.2 for V) (**12**-Co and **12**-V), was measured to be 1.2×10^{-3} and 1.6×10^{-3} S cm^{-1}, respectively, at 20 °C and 100% relative humidity.[59] A significant humidity dependence of proton conductivity was noted in **12**-Co with the proton conductivity dropping to 3.2×10^{-8} S cm^{-1} at 8% relative humidity. More interestingly, **12**-V undergoes a magnetic transition at about 310 K, which appears to have an effect on its ionic conductivity (Figure 5b) as the slope of the ln(σT) versus T plot changes at the same temperature. It is likely that the magnetic transition causes a distortion in the hydrogen-bonded network of the water molecules present in the cubic network of the Prussian blue analogue. The interference effect between ionic conductivity and magnetic ordering may be useful in designing proton-conducting switches controlled by temperature and/or external magnetic field.

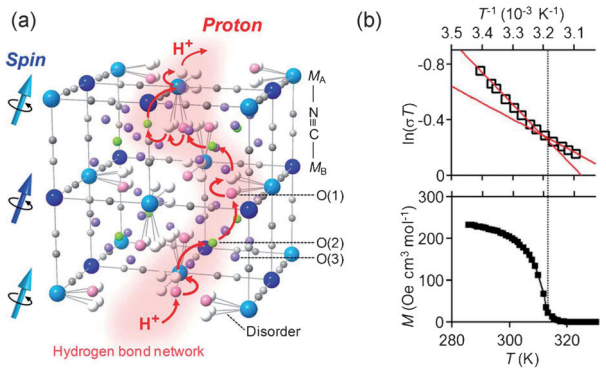

Figure 5. a) Proposed pathway for a proton transport through the hydrogen bonds between O(1), O(2), and O(3) (red arrow) in the Prussian blue analogues **12**-Co; b) ln(σT) versus T^{-1} plots at 100% relative humidity and *M* versus *T* plots of **12**-V.[59]

Recently, homochiral MOFs containing helical water chains inside were investigated for proton conduction. The enantiomeric MOFs having a zeolite *unh* topology, [Zn(*l*-L_{cl})(Cl)]·H_2O (*l*-**13**) and [Zn(*d*-L_{cl})(Cl)]·H_2O (*d*-**13**), where L = 3-methyl-2-(pyridin-4-ylmethylamino)butanoic acid, have water molecules arranged in a helical fashion within 1D channels (Figure 6).[60] As expected, *l*-**13** and *d*-**13** showed the same proton conductivity within experimental error (4.45×10^{-5} and 4.42×10^{-5} S cm^{-1}, respectively) at 30 °C and

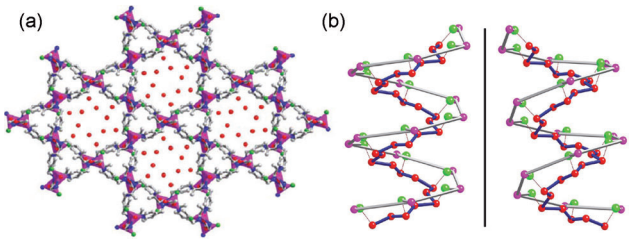

Figure 6. a) Polyhedral representation of helical MOF along the *c* axis. b) Mirror image of helical water chains in *l*-**13** and *d*-**13**.[60] Red spheres = water oxygen atoms.

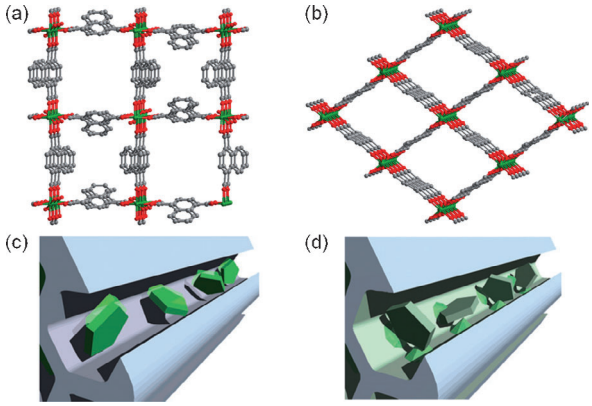

Figure 7. Aluminum-based porous frameworks for proton-conductive materials. a) Structure of **14** along the *c* axis; b) structure of **15** along the *a* axis; c) included imidazole in a nanochannel of **14** without strong host–guest interaction; d) included imidazole in a nanochannel of **15** with strong host–guest interaction.[61]

98% relative humidity. The proton conductivity exhibits a reasonable dependence on relative humidity with a value of 1.22×10^{-5} S cm^{-1} at 60% relative humidity. The activation energy for the compounds was found to be 0.35 eV.

4.2. Anhydrous Proton-Conducting MOFs

Although there are many examples of water-mediate proton conducting MOFs, their low operation temperature and humidity-dependent proton conductivity stimulated researchers to explore non-water-mediated or anhydrous proton conducting MOFs, which can operate at a higher temperature range (100–250 °C) than water-mediated proton conducting MOFs.

It has been established that the organic molecules, such as pyrazole and imidazole, when confined within the lamellar structures (inter-lamellar spaces), show interesting proton-conducting behavior.[29] Thus, replacement of water in 2D or 3D MOFs with such organic molecules would produce an interesting class of materials exhibiting proton-conducting behavior even in the absence of water molecules. Such materials are also advantageous as they may not exhibit any dependency on humidity variations.

Two heterocyclic molecules, imidazole and 1*H*-1,2,4-triazole have been incorporated as guest molecules within MOFs. Both imidazole and triazole are non-volatile and have a high boiling point ($T_b = 256$ °C and $T_b = 260$ °C, respectively). Imidazole exists in two tautomeric forms as a result of the migration of the proton between the two nitrogen atoms, thus providing a pathway for proton conduction. In addition, the imidazole and imidazolium ion pair (base–acid pair) can participate in hydrogen-bond interactions along with the possible intermolecular proton transfer. It may be noted that the solid imidazole does not exhibit significant proton conduction with a conductivity of about 10^{-8} S cm^{-1} at room temperature, but the conductivity improves appreciably near its melting temperature ($T_m = 89$ °C). Triazole also exhibits poor proton conductivity at room temperature, but good proton conductivity (1.2×10^{-3} S cm^{-1}) at the melting temperature (120 °C).

S. Kitagawa and co-workers prepared two imidazole-loaded MOFs, and investigated their proton-conduction behavior.[61] MOFs Al(μ_2-OH)(1,4-ndc) (**14**; 1,4-ndc = 1,4-naphthalenedicarboxylate),[62] and Al(μ_2-OH)(1,4-bdc) (**15**; 1,4-bdc = 1,4-benzenedicarboxylate),[54] both having 1D channels with a dimension of about 8 Å, were loaded with imidazole (Im) (Figure 7a,b). The loading of imidazole was controlled to around 0.6 imidazole per Al in **14** and 1.3 imidazole per Al in **15**. The proton conductivity at room temperature was found to be in the range of 10^{-8}–10^{-10} S cm^{-1} for both Im@**14** and Im@**15**. The proton conductivity exhibited considerable improvement at 120 °C with a value of 2.2×10^{-5} S cm^{-1} for Im@**14** and 1.0×10^{-7} S cm^{-1} for Im@**15**. The activation energy was found to be 0.6 eV for Im@**14** and 0.9 eV for Im@**15**. The large difference in conductivity as well as activation energy between the two imidazole-loaded MOFs is probably due to the difference in dynamic motion of the guest in the channels. More hydrophobic channels of **14** have weaker interaction with polar imidazole molecules, which allows the guest molecules to move freely in the channels, while the stronger interaction with more hydrophilic channels of **15** resulted in restriction in movement or rotation of the guest molecules in the framework (Figure 7c,d). This study demonstrated that MOFs can provide an appropriate pore environment and size for a target proton carrier by fine-tuning of their components.

Extending this work, S. Kitagawa and co-workers also prepared the histamine (His) loaded **14**, His@**14**, with a stoichiometry of 1.0 histamine molecule per Al^{3+} ion.[63] The proton conductivity of His@**14** linearly increased with increasing temperature from 3.0×10^{-5} S cm^{-1} at room temperature to 1.7×10^{-3} S cm^{-1} at 150 °C. The observed proton conductivity of His@**14** was higher than that for pure histamine (9.4×10^{-6} S cm^{-1}) at 75 °C. When the amount of histamine present within the channels is halved in this compound, the proton conductivity decreased to 2.1×10^{-4} S cm^{-1} at 150 °C, which suggests that the concentration of the proton carrier is critical for proton conductivity. The activation energy of proton hopping in His@**14** was estimated to be 0.25 eV. Similar to their earlier work, this study demonstrated that proton-conducting materials incorporated in MOFs show unique proton-conduction behavior, often

quite different from that in bulk, as a result of the confinement effect of being within the MOFs.

Shimizu and co-workers reported a proton-conducting MOF with channels occupied by 1*H*-1,2,4-triazole (Tz).[64] The MOF β-PCMOF-2 (**16**) based on the sulfonate-containing ligand, 2,4,6-trihydroxy-1,3,5-benzenetrisulfonate, has hexagonal sheets of the anionic ligand in the crystallographic *ab* plane cross-linked in the direction of the *c* axis by Na ions to form channels. Significantly, the channels are lined exclusively with oxygen atoms of the sulfonate groups to form a potential hydrogen-bond transfer pathway. The pristine framework exhibited temperature-dependent proton conductivity, $5\times10^{-6}\,S\,cm^{-1}$ at 30 °C and $1\times10^{-8}\,S\,cm^{-1}$ at 70 °C. The sudden drop of the conductivity above 70 °C could be due to the loss of water molecules.[15a] Triazole molecules were carefully loaded inside the 1D channels of **16** to produce β-PCMOF-2(Tz)$_x$ (Tz@**16**) with different loadings ($x=0.3$, 0.45, and 0.6). Regardless of the amount of loaded triazole, the proton conductivity of Tz@**16** at 150 °C was in the range 2–$5\times10^{-4}\,S\,cm^{-1}$ under anhydrous H_2 conditions, where the proton conduction was confirmed by the kinetic isotope effect and solid-state NMR spectroscopy. The proton conductivity of Tz@**16** was higher than that observed for either **16** or triazole itself. The activation energy depends on the amount of triazole loaded in **16**. In addition, a H_2/air cell was constructed using Tz@**16** ($x=0.45$) as a membrane, which gave an open-circuit voltage of 1.18 V, stable for 72 h at 100 °C. This study first demonstrated that the proton-conducting MOFs can be used as a fuel-cell membrane.

Because of their non-volatility, high proton conductivity, and excellent chemical and thermal stability, ionic liquids have been considered as an excellent proton-transferring medium for fuel cells.[65] Ionic-liquid-based proton-conducting membranes have thus been widely studied.[66] In addition, incorporation of ionic liquids into the pores of MOFs was recently tested to synthesize a new type of proton-conducting material. Ionic-liquid-containing MOF, $[Co_2Na(bptc)_2][Emim]_3$ (**17**), where bptc = 2,2′,4,4′-biphenyl tetracarboxylate and Emim = 1-ethyl-3-methylimidazolium, was synthesized by ionothermal synthesis.[67] It has a 3D framework with open channels occupied by imidazolium cations $(Emim)^+$. Single-crystal proton-conductivity measurements of **17** along the *c* axis (Figure 8a) and [110] direction (Figure 8b) at room temperature revealed proton conductivity of $4.78\times10^{-7}\,S\,cm^{-1}$ and $2.63\times10^{-5}\,S\,cm^{-1}$, respectively. As temperature increases, the conductivity along the *c* axis decreased, which was attributed to loss of water molecules. However, above 70 °C, proton-conductivity increased with increasing temperature and reached a maximum of $6.33\times10^{-7}\,S\,cm^{-1}$ at 170 °C. Although the proton conductivity of **17** is low compared to other MOFs, this is the first imidazolium-ion-containing MOF, prepared by ionothermal synthesis for anhydrous proton conduction.

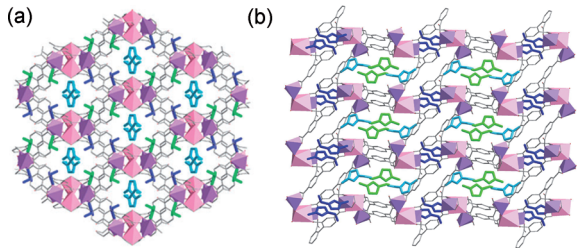

Figure 8. A channel view of **17** along a) the *c* axis and b) the [110] direction.[67]

Related to these studies, very recently, S. Kitagawa and co-workers reported a new approach to anhydrous proton-conducting MOFs. They synthesized the first intrinsic proton-conducting MOF, $[Zn(H_2PO_4)_2(TzH)_2]$ (**18**), by using triazoles and phosphates as a linker (or strut) of the MOF.[68] The coordination network is composed of octahedral Zn ions, mono-coordinated orthophosphate and bridging TzH, forming an extended 2D framework. The resulting 2D framework forms a 3D packing structure by interlayer hydrogen-bonding between triazoles and orthophosphates, which provides a proton-conduction pathway. In pellet measurements, the proton conductivity of **18** was found to be $1.2\times10^{-4}\,S\,cm^{-1}$ at 150 °C with activation energy of 0.6 eV without additional proton-conducting media. Single-crystal proton-conductivity measurements revealed that **18** shows a large anisotropic proton conduction ($\sigma_{\parallel}/\sigma_{\perp}\approx100$). This material is the first intrinsic anhydrous proton conducting MOF, which conducts protons without help of guest molecules.

Despite the remarkable progress, the development of anhydrous proton-conducting MOFs is still in its infancy. Nevertheless, the examples described herein demonstrate the possibility of developing anhydrous proton-conducting MOFs with high conductivity at a temperature between 100–250 °C.

4.3. Proton Conduction in Organic Molecular Porous Solids

Organic molecular porous solids having supramolecular architectures with pores and channels as a result of strong intermolecular interactions including hydrogen bonds among the organic building blocks, have been investigated as proton conductors. Guest molecules, such as water, are included in the channels, serving as a proton conduction pathway.

An early example was host–guest inclusion compound quinuclidine–thiourea (**19**).[69] It has a hexagonal channel structure built with hydrogen-bonded thiourea host molecules. Along the channels, quinuclidine guest molecules are included in a linear arrangement through hydrogen bonds, which paves a way for proton transport. Proton conductivity measurements using pellets revealed various quinuclidine–thiourea derivatives have conductivity of 10^{-5}–$10^{-11}\,S\,cm^{-1}$ under atmospheric conditions.[69b] Single-crystal conductivity measurements showed considerable anisotropic behavior in the proton conductivity: $2.19\times10^{-4}\,S\,cm^{-1}$ along the quinuclidine chains and $2.42\times10^{-6}\,S\,cm^{-1}$ perpendicular to the chains ($\sigma_{\parallel}/\sigma_{\perp}=\approx100$) at room temperature.[69a] The conductivity drops significantly above 40 °C. Although this was the first proton-conductivity study on organic molecular solids using single crystals, their low proton conductivity and poor stability in humid condition limits their applications.

Recently, Kim and co-workers reported the proton conductivity of cucurbituril-based organic molecular porous materials.[34] Cucurbit[*n*]urils (CB[*n*], $n=5$–8, 10) are a family

of host molecules exhibiting interesting structural arrangements in the solid state.[70] In particular, CB[6] recrystallized from dilute mineral acids such as H_2SO_4 or HCl gave compound **20** and **21**, respectively, showing honeycomb-like structures with channels occupied by water molecules and acid forming an extensive hydrogen-bonding network (Figure 9).[34,71] Proton conductivity of **20** and **21** measured using

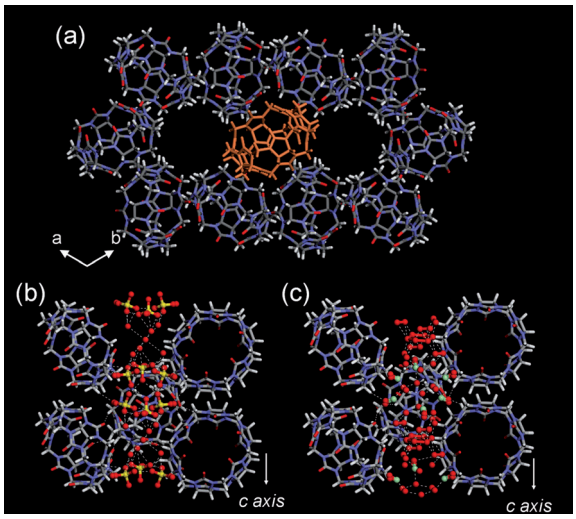

Figure 9. a) X-ray crystal structures of PCB[6] viewed along the *c*-axis. b) water-H_2SO_4 arrays filling the channels of **20**. c) water-HCl arrays in the channels of **21**.[34]

pellets was $1.3\times10^{-3}\,S\,cm^{-1}$ and $1.1\times10^{-3}\,S\,cm^{-1}$, respectively, at 25 °C and 98 % relative humidity. The conductivity was highly dependent on relative humidity, as usual, as well as on the nature and amount of acids present in the channels. Most importantly, single-crystal conductivity measurements revealed a highly anisotropic conduction behavior of the materials. The single-crystal proton conductivities of **20** and **21** along the channel direction were $4.3\times10^{-2}\,S\,cm^{-1}$ and $2.4\times10^{-2}\,S\,cm^{-1}$, respectively, which are almost 3 or 4 orders of magnitude higher than those across the channel direction ($5.0\times10^{-6}\,S\,cm^{-1}$ and 7.1×10^{-5}, respectively) This material showed the highest anisotropic proton conductivity ($\sigma_{\parallel}/\sigma_{\perp}=$ 8600) among the known proton conducting materials to date.[68,69b]

Despite some disadvantages, such as working at low temperatures and high humidity conditions, the observation of high proton conductivity in these organic molecular solids provides ample scope for investigating other self-assembled supramolecular systems.

4.4. Proton Conduction in Other Porous Materials

The earliest and most established porous materials are the aluminosilicate zeolites, which have considerable advantages because of their high thermal stability and acidity. Proton conductivity in zeolites could arise from the presence of a proton conducting species, such as H_3O^+ and NH_4^+, in pores of zeolites as countercations.[72] It should be noted that earlier studies on metal phosphonates suggests that acid functional groups, such as sulfonates, enhances the proton conductivity of zeolites.[73] Similar to this, acid functionalization of the zeolite surface is also advantageous for high proton conductivity ($10^{-4}\,S\,cm^{-1}$).[74] Recently, Davis and co-workers incorporated phenyl sulfonic acid groups into hydrophilic zeolite beta, which gave an increase in proton conductivity to $5\times10^{-3}\,S\,cm^{-1}$.[75] This change may be due to the increased hydrophilicity of the pores, as the formation of a hydrogen-bonded water network is important for fast proton hopping.

Similar to zeolites, mesoporous silica[76] was surface-functionalized with phosphonate and sulfonate groups which provide a proton conduction pathway. Mesoporous silica containing phosphonate functional groups showed a conductivity of around $10^{-2}\,S\,cm^{-1}$ at 100–120 °C and 100 % relative humidity, which is higher than that pristine mesoporous silica (ca. $10^{-4}\,S\,cm^{-1}$).[77] Another mesoporous silica, Si-MCM-41, having sulfonate groups on the surface of the pores showed a conductivity of $0.2\,S\,cm^{-1}$ at room temperature and 100 % relative humidity, which is considerably higher than the $10^{-6}\,S\,cm^{-1}$ observed for pristine Si-MCM-41.[78]

Nanomaterials hold an important place in the today's science. The usefulness of some of the nanomaterials is beginning to emerge and there have been studies on possible proton-conduction in nanotubular arrays. Molecular simulation studies suggested facile proton conduction in carbon nanotubes filled with water molecules.[79] However, an experimental demonstration of proton conductivity by carbon nanotubes has not yet been reported. Another type of nanotubes, metal oxide nanotubes formed from titanate ($H_2Ti_3O_7$), showed a reasonable proton conductivity of $5\times10^{-4}\,S\,cm^{-1}$ at 160 °C and 100 % relative humidity.[80] A low activation energy (0.09 eV) suggested a hopping mechanism through hydrogen-bonded water network that fills the channels of the nanotubes.

5. Other Ion Conduction in MOFs

For energy-related purposes, though fuel-cells appear to be attractive, those based on ionic mobility such as Li^+ conduction is equally attractive. One drawback that lithium-ion batteries suffer from is the availability of good quality solid electrolyte materials as most of them have Li^+ salts dissolved in organic carbonates as the electrolyte. The use of liquid- or gel-based electrolytes in lithium-ion batteries impose restrictions on the shape, processing, as well as operation temperature of the batteries. As the ionic conduction in porous materials is facilitated by having a suitable conduit for the mobility of ions, an interesting twist to the proton conduction in porous materials, is to investigate the mobility of ions that are small, such as Li^+ ions. It would really open the usage of Li batteries in energy-demanding applications, such as electric vehicles. This is an area that may possess possible future in the applications of porous materials.

Recently, Long and co-workers explored the Li^+ ion conduction in MOFs having open coordination sites, Mg_2-(dobdc),[81] where dobdc = 1,4-dioxido-2,5-benzenedicarboxylate (**22**).[82] The structure of **22** consists of 1D hexagonal

channels that are lined with open coordination sites (OCS). Incorporation of alkoxide anions into **22**, which preferentially binds to the open coordination sites of Mg ions, pin the alkoxides in place while leaving the Li^+ ions relatively free to move along the channels. The new electrolyte, Mg_2-(dobdc)·0.35 LiO*i*Pr·0.25 $LiBF_4$·EC·DEC, where EC = ethylenecarbonate and DEC = diethylcarbonate (**22**-Li), exhibited a conductivity of 3.1×10^{-4} S cm^{-1} at 300 K under anhydrous condition. The activation energy for the Li^+ conduction was 0.15 eV. In addition, **22**-Li can also be processed into polycrystalline solid thin films, which showed a conductivity of 5.5×10^{-4} S cm^{-1}. The clever use of Mg along with Li provides new vistas for the use of modified porous materials as an electrolyte in Li batteries, and opens enormous possibilities in this area. Although this is the only example of Li ion conduction in MOFs, a bright future is anticipated for the exploration of MOFs and other porous materials in conduction of ions such as Li and Na.

6. Summary and Perspectives

Herein, we surveyed the proton-conduction properties of several MOFs and related modular porous solids. It is clear that the proton conductivity in water-mediated proton conducting MOFs depends on water-based hydrogen-bonding arrays or networks, which offer a proton-conduction pathway. Anhydrous proton-conducting MOFs having occluded molecules, such as imidazole and triazole, exhibit good to excellent proton conductivity under anhydrous condition even at higher temperature (up to around 150 °C). Although the examples of anhydrous proton-conducting coordination polymers are limited, they are attractive for use in hydrogen fuel-cell related technologies. Similar to water-mediated proton-conducting MOFs, organic molecular porous solids also showed high proton conductivity at low temperatures and high humidity conditions.

Despite the recent progresses in proton conducting MOFs and related modular porous solids, many challenges as well as opportunities still remain. The design flexibility and framework tunability of this class of materials suggest that they can serve as a versatile platform for new types of proton-conducting materials. For example, incorporation of stimuli responsive units into a MOF framework, the channels of which are filled with proton conducting media, would allow control of the proton conductivity by applying external stimuli, which may be applicable to design a proton-conduction-based switch. In addition, judicious selection of pore surface functionality and/or included guest molecules allows fine tuning of proton conductivity of such modular porous solids. Furthermore, their crystalline nature may provide unique opportunities to study the mechanism of proton conduction by utilizing the structural characterization of key intermediates involved in proton conduction using in situ crystallography or time-resolved X-ray diffraction techniques. Although their poor processibility is a serious problem, recent efforts to synthesize MOF thin films may provide new opportunities for their applications. With this great potential, proton-conducting modular porous solids will likely become, in the next decade, one of the important class of materials in electrochemical devices and proton sensors involved in high proton conductivity and precisely controlled proton conductivity, respectively.

We gratefully acknowledge the Acceleration Research, BK 21, and WCU program (Project No. R31-2008-000-10059-0) of the National Research Foundation of Korea (to K.K.) and Department of Science and Technology of India for the award of Rammanna Fellowship (to S.N.) for the support of the research at POSTECH

Received: August 9, 2012
Revised: October 22, 2012
Published online: January 23, 2013

[1] A. Volta, *Phil. Trans.* **1782**, *72*, 237 – 283.
[2] G. D. Scholes, G. R. Fleming, A. Olaya-Castro, R. van Grondelle, *Nat. Chem.* **2011**, *3*, 763 – 774.
[3] G. W. Crabtree, M. S. Dresselhaus, *MRS Bull.* **2008**, *33*, 421 – 428.
[4] a) S. J. Paddison, *Annu. Rev. Mater. Res.* **2003**, *33*, 289 – 319; b) S. J. Peighambardoust, S. Rowshanzamir, M. Amjadi, *Int. J. Hydrogen Energy* **2010**, *35*, 9349 – 9384.
[5] a) "Proton Conductors: Solids, Membranes and Gels-Materials and Devices": P. Colomban in *Chemistry of Solid State Materials*, *Vol. 2*, Cambridge University Press, Cambridge, **1992**; b) K. D. Kreuer, *Chem. Mater.* **1996**, *8*, 610 – 641; c) K. D. Kreuer, S. J. Paddison, E. Spohr, M. Schuster, *Chem. Rev.* **2004**, *104*, 4637 – 4678.
[6] A special issues on MOFs, a) *Chem. Soc. Rev.* **2009**, *38*, 1201 – 1508; b) *Eur. J. Inorg. Chem.* **2010**, 3683 – 3874; c) *Chem. Rev.* **2012**, *112*, 673 – 1268.
[7] Herein we use the terms 1D CPs, 2D MOFs, and 3D MOFs, by following the terminology guidelines of coordination compounds recently suggested, S. R. Batten, N. R. Champness, X.-M. Chen, J. Garcia-Martinez, S. Kitagawa, L. Öhrström, M. O'Keeffe, M. P. Suh, J. Reedijk, *CrystEngComm* **2012**, *14*, 3001 – 3004.
[8] a) S. J. Dalgarno, P. K. Thallapally, L. J. Barbour, J. L. Atwood, *Chem. Soc. Rev.* **2007**, *36*, 236 – 245; b) J. R. Holst, A. Trewin, A. I. Cooper, *Nat. Chem.* **2010**, *2*, 915 – 920; c) J. T. A. Jones, D. Holden, T. Mitra, T. Hasell, D. J. Adams, K. E. Jelfs, A. Trewin, D. J. Willock, G. M. Day, J. Bacsa, A. Steiner, A. I. Cooper, *Angew. Chem.* **2011**, *123*, 775 – 779; *Angew. Chem. Int. Ed.* **2011**, *50*, 749 – 753.
[9] a) C. J. T. van Grotthuss, *Ann. Chim.* **1806**, *58*, 54 – 73; b) S. Cukierman, *Biochim. Biophys. Acta Bioenerg.* **2006**, *1757*, 876 – 885; c) N. Agmon, *Chem. Phys. Lett.* **1995**, *244*, 456 – 462.
[10] W. E. Ayrton, J. Perry, *Proc. Phys. Soc. London* **1877**, *2*, 171 – 182.
[11] W. Bjerrum, *Science* **1952**, *115*, 385 – 390.
[12] M. Eigen, L. De Maeyer, H.-Ch. Sparz, *Ber. Bunsen-Ges.* **1964**, *68*, 19 – 29.
[13] F. M. Ernsberger, *J. Am. Ceram. Soc.* **1983**, *66*, 747 – 750.
[14] a) See Ref. [9c]; b) N. Agmon, *J. Chim. Phys.* **1996**, *93*, 1714 – 1736; c) M. E. Tuckerman, D. Marx, M. Parrinello, *Nature* **2002**, *417*, 925 – 929; d) T. C. Berkelbach, H.-S. Lee, M. E. Tuckerman, *Phys. Rev. Lett.* **2009**, *103*, 238302; e) Z. Ma, M. E. Tuckerman, *Chem. Phys. Lett.* **2011**, *511*, 177 – 182.
[15] a) K. A. Mauritz, R. B. Moore, *Chem. Rev.* **2004**, *104*, 4535 – 4585; b) S. S. Ivanchev, *Russ. J. Appl. Chem.* **2008**, *81*, 569 – 584; c) T. D. Gierke, G. E. Munn, F. C. Wilson, *J. Poly. Sci. B* **1981**, *19*, 1687 – 1704;

[16] a) Y. Wang, K. S. Chen, J. Mishler, S. C. Cho, X. C. Adroher, *Appl. Energy* **2011**, *88*, 981 – 1007; b) M. Rikukawa, K. Sanui, *Prog. Polym. Sci.* **2000**, *25*, 1463 – 1502.

[17] There is no clear-cut definition of a good conductor available in the literature. However, proton conductivity of more than 0.1 $mS\,cm^{-1}$ can be considered as high conductivity as Colomban and co-workers defined the superionic conductor in a Review article (Ref. [5a]).

[18] L. Glasser, *Chem. Rev.* **1975**, *75*, 21 – 65.

[19] a) D. A. Shores, R. A. Rapp, *J. Electrochem. Soc.* **1972**, *119*, 300 – 305; b) K. D. Kreuer, *Annu. Rev. Mater. Res.* **2003**, *33*, 333 – 359.

[20] a) T. Takahashi, H. Iwahara, *Rev. Chim. Miner.* **1980**, *17*, 243 – 305; b) K. D. Kreuer, *Solid State Ionics* **1999**, *125*, 285 – 302.

[21] T. Norby, O. Dryli, P. Kofstad, *J. Am. Ceram. Soc.* **1992**, *75*, 1176 – 1181.

[22] T. Dippel, K. D. Kreuer, J. C. Lassègues, D. Rodriguez, *Solid State Ionics* **1993**, *61*, 41 – 46.

[23] A. Potier, D. Rousselet, *J. Chim. Phys.* **1973**, *70*, 873 – 879.

[24] R. A. Munson, *J. Phys. Chem.* **1964**, *68*, 3374 – 3380.

[25] a) A. J. Baranov, L. A. Shuvalov, N. M. Shchagina, *JETP Lett.* **1982**, *36*, 459 – 462; b) G. Alberti, E. Torracca, *J. Inorg. Nucl. Chem.* **1968**, *30*, 1093 – 1099; c) A. Goñi-Urtiaga, D. Presvytes, K. Scott, *Int. J. Hydrogen Energy* **2012**, *37*, 3358 – 3372.

[26] T. Takahashi, S. Tanase, O. Yamamoto, S. Yamauchi, *J. Solid State Chem.* **1976**, *17*, 353 – 361.

[27] S. Chandra, S. A. Hashmi, G. Prasad, *Solid State Ionics* **1990**, *40/41*, 651 – 654.

[28] J. A. Asensio, E. M. Sánchez, P. Gómez-Romero, *Chem. Soc. Rev.* **2010**, *39*, 3210 – 3239.

[29] a) G. Alberti, U. Constantino, M. Casciola, R. Vivani, A. Peraio, *Solid State Ionics* **1991**, *46*, 61 – 68; b) K. D. Kreuer, A. Fuchs, M. Ise, M. Spaeth, J. Maier, *Electrochim. Acta* **1998**, *43*, 1281 – 1288; c) W. Münch, K. D. Kreuer, W. Silvestri, J. Maier, G. Seifert, *Solid State Ionics* **2001**, *145*, 437 – 443.

[30] N. Azuma, R. Ohtsuka, Y. Morioka, H. Kosugi, J. Kobayashi, *J. Mater. Chem.* **1991**, *1*, 989 – 996.

[31] D. E. Katsoulis, *Chem. Rev.* **1998**, *98*, 359 – 388.

[32] T. Norty, *Solid State Ionics* **1999**, *125*, 1 – 11.

[33] X.-Z. Yuan, C. Song, H. Wang, J. Zhang, *Electrochemical Impedance Spectroscopy in PEM Fuel Cells*, Springer, London, **2010**, pp. 201 – 212.

[34] M. Yoon, K. Suh, H. Kim, Y. Kim, N. Selvapalam, K. Kim, *Angew. Chem.* **2011**, *123*, 8016 – 8019; *Angew. Chem. Int. Ed.* **2011**, *50*, 7870 – 7873.

[35] S. Kanda, K. Yamashita, K. Ohkawa, *Bull. Chem. Soc. Jpn.* **1979**, *52*, 3296 – 3301.

[36] Reviews: a) L. J. Murray, M. Dincă, J. R. Long, *Chem. Soc. Rev.* **2009**, *38*, 1294 – 1314; b) K. Sumida, D. L. Rogow, J. A. Mason, T. M. McDonald, E. D. Bloch, Z. R. Herm, T.-H. Bae, J. R. Long, *Chem. Rev.* **2012**, *112*, 724 – 781; c) M. P. Suh, H. J. Park, T. K. Prasad, D. W. Lim, *Chem. Rev.* **2012**, *112*, 782 – 835.

[37] Reviews: a) J.-R. Li, R. J. Kuppler, H.-C. Zhou, *Chem. Soc. Rev.* **2009**, *38*, 1477 – 1504; b) J. R. Li, J. Sculley, H.-C. Zhou, *Chem. Rev.* **2012**, *112*, 869 – 932.

[38] Reviews: a) L. Ma, C. Abney, W. Lin, *Chem. Soc. Rev.* **2009**, *38*, 1248 – 1256; b) J. Y. Lee, O. K. Farha, J. Roberts, K. A. Scheidt, S. T. Nguyen, J. T. Hupp, *Chem. Soc. Rev.* **2009**, *38*, 1450 – 1459; c) K. Kim, M. Banerjee, M. Yoon, S. Das, *Top. Curr. Chem.* **2010**, *293*, 115 – 153; d) M. Yoon, R. Srirambalaji, K. Kim, *Chem. Rev.* **2012**, *112*, 1196 – 1231.

[39] a) G. J. Halder, C. J. Kepert, B. Moubaraki, K. S. Murray, J. D. Cashion, *Science* **2002**, *298*, 1762 – 1765; b) M. Kurmoo, *Chem. Soc. Rev.* **2009**, *38*, 1353 – 1379.

[40] T. Yamada, M. Sadakiyo, H. Kitagawa, *J. Am. Chem. Soc.* **2009**, *131*, 3144 – 3145.

[41] a) S. Morikawa, T. Yamada, H. Kitagawa, *Chem. Lett.* **2009**, *38*, 654 – 655; b) T. Yamada, S. Morikawa, H. Kitagawa, *Bull. Chem. Soc. Jpn.* **2010**, *83*, 42 – 48.

[42] C. Dey, T. Kundu, R. Banerjee, *Chem. Commun.* **2012**, *48*, 266 – 268.

[43] T. Panda, T. Kundu, R. Banerjee, *Chem. Commun.* **2012**, *48*, 5464 – 5466.

[44] a) S. Kanda, F. Yamamoto, *Bull. Chem. Soc. Jpn.* **1996**, *69*, 477 – 483; b) T. Yamada, R. Yonamine, T. Yamada, H. Kitagawa, O. Yamamuro, *J. Phys. Chem. B* **2010**, *114*, 8405 – 8409.

[45] H. Kitagawa, Y. Nagao, M. Fujishima, R. Ikeda, S. Kanda, *Inorg. Chem. Commun.* **2003**, *6*, 346 – 348.

[46] a) Y. Nagao, R. Ikeda, S. Kanda, Y. Kubozono, H. Kitagawa, *Mol. Cryst. Liq. Cryst.* **2003**, *379*, 89 – 94; b) Y. Nagao, M. Fujishima, R. Ikeda, S. Kanda, H. Kitagawa, *Synth. Met.* **2003**, *133 – 134*, 431 – 432; c) Y. Nagao, R. Ikeda, K. Iijima, T. Kubo, K. Nakasuji, H. Kitagawa, *Synth. Met.* **2003**, *135 – 136*, 283 – 284; d) Y. Nagao, T. Kubo, K. Nakasuji, R. Ikeda, T. Kojima, H. Kitagawa, *Synth. Met.* **2005**, *154*, 89 – 92.

[47] H. Tamaki, Z. J. Zhong, N. Matsumoto, S. Kida, M. Koikawa, N. Achiwa, Y. Hashimoto, H. Okawa, *J. Am. Chem. Soc.* **1992**, *114*, 6974 – 6979.

[48] M. Sadakiyo, T. Yamada, H. Kitagawa, *J. Am. Chem. Soc.* **2009**, *131*, 9906 – 9907.

[49] H. Okawa, A. Shigematsu, M. Sadakiyo, T. Miyagawa, K. Yoneda, M. Obha, H. Kitagawa, *J. Am. Chem. Soc.* **2009**, *131*, 13516 – 13522.

[50] M. Sadakiyo, H. Okawa, A. Shigematsu, M. Ohba, T. Yamada, H. Kitagawa, *J. Am. Chem. Soc.* **2012**, *134*, 5472 – 5475.

[51] E. Pardo, C. Train, G. Gontard, K. Boubekeur, O. Fabelo, H. Liu, B. Dkhil, F. Lloret, K. Nakagawa, H. Tokoro, S.-i. Ohkoshi, M. Verdaguer, *J. Am. Chem. Soc.* **2011**, *133*, 15328 – 15331.

[52] R. Yu, L. C. De Jonghe, *J. Phys. Chem. C* **2007**, *111*, 11003 – 11007.

[53] J. M. Taylor, R. K. Mah, I. L. Moudrakovski, C. I. Ratcliffe, R. Vaidhyanathan, G. K. H. Shimizu, *J. Am. Chem. Soc.* **2010**, *132*, 14055 – 14057.

[54] C. Serre, F. Millange, C. Thouvenot, M. Nogués, G. Marsolier, D. Louër, G. Férey, *J. Am. Chem. Soc.* **2002**, *124*, 13519 – 13526.

[55] A. Shigematsu, T. Yamada, H. Kitagawa, *J. Am. Chem. Soc.* **2011**, *133*, 2034 – 2036.

[56] L. P. Hammett, *J. Am. Chem. Soc.* **1937**, *59*, 96 – 103.

[57] S. S. Y. Chui, S. M. F. Lo, J. P. H. Charmant, A. G. Orpen, I. D. Williams, *Science* **1999**, *283*, 1148 – 1150.

[58] N. C. Jeong, B. Samanta, C. Y. Lee, O. K. Farha, J. T. Hupp, *J. Am. Chem. Soc.* **2012**, *134*, 51 – 54.

[59] S.-I. Ohkoshi, K. Nakagawa, K. Tomono, K. Imoto, Y. Tsunobuchi, H. Tokoro, *J. Am. Chem. Soc.* **2010**, *132*, 6620 – 6621.

[60] S. C. Sahoo, T. Kundu, R. Banerjee, *J. Am. Chem. Soc.* **2011**, *133*, 17950 – 117968.

[61] S. Bureekaew, S. Horike, M. Higuchi, M. Mizuno, T. Kawamura, D. Tanaka, N. Yanai, S. Kitagawa, *Nat. Mater.* **2009**, *8*, 831 – 836.

[62] A. Comotti, S. Bracco, P. Sozzani, S. Horike, R. Matsuda, J. Chen, M. Takata, Y. Kubota, S. Kitagawa, *J. Am. Chem. Soc.* **2008**, *130*, 13664 – 13672.

[63] D. Umeyama, S. Horike, M. Inukai, Y. Hijikata, S. Kitagawa, *Angew. Chem.* **2011**, *123*, 11910 – 11913; *Angew. Chem. Int. Ed.* **2011**, *50*, 11706 – 11709.

[64] J. A. Hurd, R. Vaidhyanathan, V. Thangadurai, C. I. Ratcliffe, I. L. Moudrakovski, G. K. H. Shimizu, *Nat. Chem.* **2009**, *1*, 705 – 710.

[65] *Ionic Liquids: The Front and Future of Material Development* (Ed.: H. Ohno), CMC, Tokyo, **2003**.

[66] a) S. Subianto, M. K. Mistry, N. R. Choudhury, N. K. Dutta, R. Knott, *ACS Appl. Mater. Interfaces* **2009**, *1*, 1173 – 1182; b) S. Yu, F. Yan, X. Zhang, J. You, P. Wu, J. Lu, Q. Xu, X. Xia, G. Ma, *Macromolecules* **2008**, *41*, 3389 – 3392; c) F. Yan, S. Yu, X.

Zhang, L. Qiu, F. Chu, J. You, J. Lu, *Chem. Mater.* **2009**, *21*, 1480 – 1484.
[67] W. X. Chen, H.-R. Xu, G.-L. Zhuang, L.-S. Long, R.-B. Huang, L. S. Zheng, *Chem. Commun.* **2011**, *47*, 11933 – 11935.
[68] D. Umeyama, S. Horike, M. Inukai, T. Itakura, S. Kitagawa, *J. Am. Chem. Soc.* **2012**, *134*, 12780 – 12785.
[69] a) J. Merchan, V. Lavayen, P. Jara, V. Sanchez, N. Yutronic, *J. Chil. Chem. Soc.* **2008**, *53*, 1498 – 1502; b) N. Yutronic, J. Merchan, P. Jara, V. Manriquez, O. Witke, G. Gonzalez, *Supramol. Chem.* **2004**, *16*, 411 – 414.
[70] Review: J. W. Lee, S. Samal, N. Selvapalam, H.-J. Kim, K. Kim, *Acc. Chem. Res.* **2003**, *36*, 621 – 630.
[71] S. Lim, H. Kim, N. Selvapalam, K.-J. Kim, S. J. Cho, G. Seo, K. Kim, *Angew. Chem.* **2008**, *120*, 3400 – 3403; *Angew. Chem. Int. Ed.* **2008**, *47*, 3352 – 3355.
[72] a) K. D. Kreuer, W. Weppener, A. Rabenau, *Mater. Res. Bull.* **1982**, *17*, 501 – 508; b) "Proton Conductors: Solids, Membranes and Gels-Materials and Devices": P. Colomban in *Chemistry of Solid State Materials*, *Vol. 2*, Cambridge University Press, Cambridge, **1992**, pp. 210 – 223.
[73] a) G. Alberti, M. Casciola, R. Palombari, A. Peraio, *Solid State Ionics* **1992**, *58*, 339 – 344; b) E. W. Stein, A. Clearfield, M. A. Subramanian, *Solid State Ionics* **1996**, *83*, 113 – 124; c) "Metal Organophosphonate Proton Conductors": G. K. H. Shimizu, J. M. Taylor, K. W. Dawson in *Metal Phosphonate Chemistry: From Synthesis to Applications* (Ed.: A. Clearfield, K. Demadis), Royal Society of Chemistry, Cambridge, **2011**, pp. 493 – 524.
[74] J. C. McKeen, Y. S. Yan, M. E. Davis, *Chem. Mater.* **2008**, *20*, 5122 – 5124.
[75] J. C. McKeen, Y. S. Yan, M. E. Davis, *Chem. Mater.* **2008**, *20*, 3791 – 3793.
[76] a) F. Hoffmann, M. Cornelius, J. Morell, M. Früba, *Angew. Chem.* **2006**, *118*, 3290 – 3328; *Angew. Chem. Int. Ed.* **2006**, *45*, 3216 – 3251; b) B. Naik, N. N. Ghosh, *Recent Pat. Nanotechnol.* **2009**, *3*, 213 – 224.
[77] S. Suzuki, Y. Nozaki, T. Okumura, M. Miyayama, *J. Ceram. Soc. Jpn.* **2006**, *114*, 303 – 307.
[78] R. Marschall, J. Rathousky, M. Wark, *Chem. Mater.* **2007**, *19*, 6401 – 6407.
[79] D. J. Mann, M. D. Halls, *Phys. Rev. Lett.* **2003**, *90*, 195503.
[80] M. Yamada, M. Wei, I. Honma, H. Zhou, *Electrochem. Commun.* **2006**, *8*, 1549 – 1552.
[81] S. R. Caskey, A. G. Wong-Foy, A. J. Matzger, *J. Am. Chem. Soc.* **2008**, *130*, 10870 – 10871.
[82] B. M. Wiers, M.-L. Foo, N. P. Balsara, J. R. Long, *J. Am. Chem. Soc.* **2011**, *133*, 14522 – 14525.